MATERIALS
&
METHODOLOGY

8.0. Data used

8.1. Reference Maps:

The Survey of India (SOI), topographical maps at 1:50,000 scales was used as a reference map for the base map preparation. Besides, SOI Toposheet, maps provided by forest department was used for digitizing district boundary as well as village boundaries.

8.1.1. Satellite Data:

8.1.1.1. Optical Data

Table A-Displaying optical data

Sr. No	Data used	Path/ Row	Date of data acquisition	Wavelength width in µm/ band	Spatial resolution (m)	Swath (km)
1	Landsat-TM	148/045	19th October 1990	0.45-0.52 (blue) 0.52-0.60 (green) 0.63-0.69 (red) 0.76-0.90 (NIR) 1.55-1.75 (SWIR) 10.4-12.5 (thermal IR) 2.08-2.35 (SWIR)	30m (120m -thermal)	185 km
2	Landasat ETM+	148/045	11th November, 2001	0.45-0.515 (blue) 0.525-0.605 (green) 0.63-0.690 (red) 0.75-0.90 (NIR) 1.55-1.75 (SWIR) 10.40-12.5 (thermal IR) 2.09-2.35 (SWIR) 0.52-0.90 (pan)	30m (60m-thermal, 15m pan)	183 km
3	IRS- 1C, 1D LISS III	99/ (54,55) 100/ (54,55)	16-November 1997, November 2005	0.52-0.59 (green) 0.62-0.68 (red) 0.77-0.86 (NIR) 1.55-1.70 (MIR)	23.5	141

8.1.1.1.1. Landsat-TM Data:

The Thematic Mapper (TM) is an advanced, multispectral scanning, Earth resources sensor designed to achieve higher image resolution, sharper spectral separation, improved geometric fidelity and greater radiometric accuracy and resolution than the MSS sensor. TM data are sensed in seven spectral bands simultaneously. Band 6 senses thermal (heat) infrared radiation. Landsat can only acquire night scenes in band 6. A TM scene has an Instantaneous Field Of View (IFOV) of 30 square meters in bands 1-5 and 7 while band 6 has an IFOV of 120 square meters on the ground.

8.1.1.1.2. Landasat ETM^{+}:

The Enhanced Thematic Mapper Plus (ETM+) instrument is a fixed "whisk-broom", eight-band, multispectral scanning radiometer capable of providing high-resolution imaging information of the Earth's surface. It detects spectrally filtered radiation in VNIR, SWIR, LWIR, and panchromatic bands from the sun-lit Earth in a 183 km wide swath when orbiting at an altitude of 705 km. An ETM+ scene has an Instantaneous Field Of View (IFOV) of 30 meters in bands 1-5 and 7 while band 6 has an IFOV of 60 meters on the ground and the band 8, an IFOV of 15 meters.

8.1.1.1.3. IRS LISS III:

LISS - III camera provides multispectral data in 4 bands. The spatial resolution for visible (two bands) and near infrared (one band) is 23.5 meters with a ground swath of 141 kms. The fourth band (short wave infrared band) has a spatial resolution of 70.5 meters with a ground swath of 148 kms. The repetitivity of LISS - III is 24 days.

8.1.1.2. Microwave data:

Table B Displaying Microwave data

Sr. No	Product	Date	Beam	Band	Polarization
1	**ENVISAT ASAR-ASA-APP**			**C**	**VV/HH**
2	**RADARSAT-2**	**February 2011 April 2011 June 2011**	**FQ4 HH VV HV VH**	**C**	**VV,HV,VH, HH**

8.1.1.2.1. ENVISAT Advanced Synthetic Aperture Radar (ASAR):

The ASAR is an advanced version of the synthetic aperture radar from the ERS-1 and 2 missions. It operates at 5.331GHz and incorporates a number of imaging modes that provide a variety of resolutions, polarizations and swath widths. Generally, the swath width is 100 km with the exception of wave mode (5 km) and the wide swath width and global monitoring (400 km) products.

8.1.1.2.2. ASAR Alternating Polarization Precision Image:

ASAR data product is generated from Level 0 data, collected when the instrument is in Alternating Polarization Mode (7 possible swaths). The product contains two

CO-registered images corresponding to one of the three polarization combination submodes (HH and VV, HH and HV, VV and VH). The distinct features are as follows:

- Coverage-100 km along-track, 56-100 km across-track
- Geometric resolution -Approximately 30m ground range * 30m azimuth
- Radiometric resolution - Product ENL > 1.8
- Pixel spacing **-12.5m * 12.5m**

8.1.1.2.3. RADARSAT-2:

RADARSAT-2, launched in 2007, is a SAR satellite developed by the Canadian Space Agency and MacDonald, Dettwiler, and Associates, Ltd. (MDA). The satellite advancements include 3 meter high-resolution imaging, flexibility in polarization selection, left and right-looking imaging options, and superior data storage. In addition to RADARSAT-1, beam modes, RADARSAT-2 offers Ultra- Fine, Multi-Look Fine, Fine Quad-Pol, and Standard Quad-Pol beam modes. Quadrate-polarization means that four images are acquired simultaneously; two co-polarized images (HH and VV) and two cross polarized images (HV and VH).

Flow-chart 1--Forest Inventory

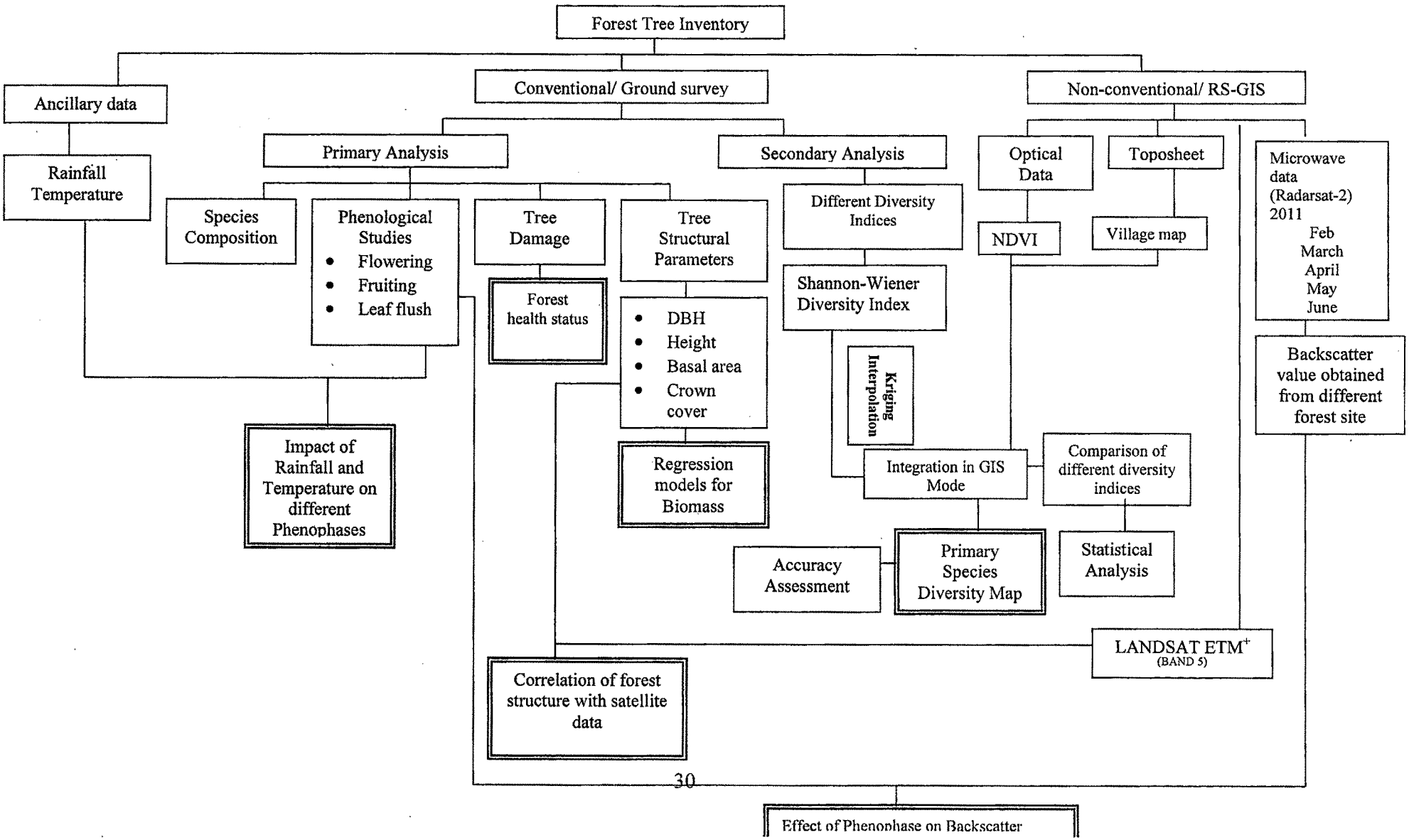

9.0. Ground survey:

The ground survey involved detailed reconnaissance of the forest area to understand the species composition, phenological status of the forest, levels of damage to the forest area and assessment of different tree structural parameters.

Information comparison and need of each feature is essential for tree inventory and it has been brought out separately.

9.1. Primary analysis:

Primary analysis consisted of understanding the tree diversity, phenological status and evaluating the tree structural parameter.

9.1.1. Tree composition:

Tree composition was assessed to understand the Tree diversity composition of Dediapada Taluka.

9.1.2. Phenology:

The Phenological observations of tree species were carried out at ground level. Phenology chart was prepared based on the Frequency of flowering, fruiting and Leaf flush of each tree species in a particular month this was carried out by frequent field visit for year 2007. In addition to these the previous records of Phenology for the year 1992 (Sabnis and Amin,1992) was taken and comparison for both the year was carried out.

9.1.3. Tree structural parameter:

Assessment of Tree structural has been carried out in five different villages of Dediapada Taluka. For tree species, belt transect (20 m X 10m) was laid down in three replicates at each site.

1. **DBH-** DBH of trees was measured using diameter tape at a height of 1.4 m (or 4' 6")

from the ground level and correspondingly the basal area was calculated.

2. **Average crown spread** was measured as per the method given by Banks *et al.* (1999). In each transect all the stems having 30 cm and above girth were considered as trees (Pande, 2006).
3. **Basal area (BA)** of individual tree and Total Basal Area (TBA) of different tree species in the forest were calculated as follows:

$$BA\ (cm^2) = (GBH/2\pi)^2 \times \pi$$

$$TBA\ (in\ m^2\ per\ ha) = \sum BA/10{,}000$$

4. **Tree Height:**

Tree height was calculated using a Blume Leiss clinometer. This instrument uses the principle of Trigonometry illustrated in Illustration 1. One measurement is made at the tree top, another at the stem base. The two angles a1 and a2 are read, and the distance of the observer from the tree, *D*, is measured. The tree height is then determined from these three known variables accordingly the formula for tree height is as given below:

H=AB =BC+CA

Where, BC = *D* tan α_1, and CA=*D* tan α_2, and so,

AB=*D* (tan α_1 +tan α_2.).

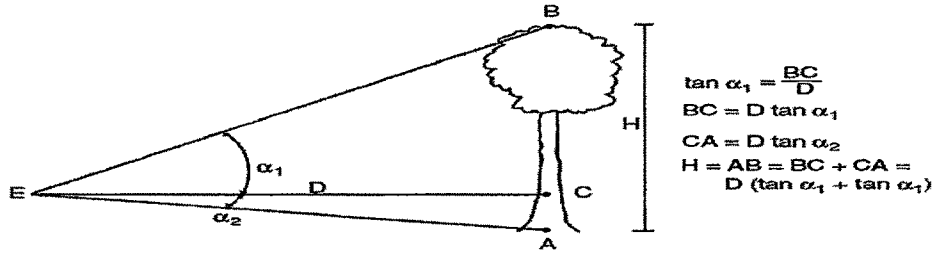

Illustration 1: Height measurements: trigonometric principle

9.2. Secondary analysis:

Field data were subjected to various ecological methods for assessment of the species diversity. Different indices were used to show the species compositional package. Different indices studied are listed as below:

9.2.1. Shannon-Wiener Diversity Index -Shannon in 1948

$$H' = -\Sigma [(ni / N) \times (\ln ni / N)]$$

H': Shannon Diversity Index, ni : Number of individuals belonging to i species,

N : Total number of individuals

9.2.2. Margalef Index-Margalef 1957

$$d = (S-1) / \ln N$$

d : Margalef Diversity Index

S : Total number of species

N : Total number of individuals

9.2.3. McIntosh Index- It was suggested by McIntosh in 1967.

$$Mc = [N - \sqrt{(\sum n_i^2)}] / [N - \sqrt{N}]$$

Mc : McIntosh Diversity Index

ni : Number of individuals belonging to i species

N : Total number of individual

9.2.4. Brillouin index -Pielou 1975.

The Brillouin index, HB, is calculated using:

$$HB = \frac{\ln N! - \sum_{i=1}^{s} \ln n_i!}{N}$$

N is the total number of individuals in the sample, ni is the number of individuals

belonging to the i^{th} species and s the species number

9.3. Non-Conventional:

Non conventional techniques like remote sensing (RS)and Geographical information system (GIS) were used to assess the species diversity, Phenology and tree structural parameters.

9.3.1. Species diversity assessment:

IRS_P3 LISS-III of Nov-2005 data, Normalized Differential Vegetation Index (NDVI) Map was generated using ERDAS-9.1. Different maps viz, NDVI, and Village (generated from the cadastral map) were converted into digital format with help of ArcGIS-9.1. The information on tree diversity collected from the ground was then integrated with spatial information in gis mode to generated diversity map. The geostatistical Kriging interpolation technique was generated for the Shannon Index. Accuracy of the Kriging interpolation technique was then carried out to validate the result.

9.3.2. Phenological assessment:

Backscatter values from Radarsat-2 were retrieved using Next ESA SAR Toolbox (NEST) 4A software for the period of five months (February to June). Backscatter values were also plotted for quad-pol for five months.

9.3.3. Regression analysis:

Relationships between DBH, Total Height and Canopy Cover of the following trees, viz. *Tectona grandis* Linn. *Butea monosperma* (Lam.) Taub., *Dalbergia sissoo* Roxb. ex DC. *Madhuca longifolia* (J.Konig) J.F.Macbr., and *Terminalia crenulata* Roth were carried out.

9.3.4. Tree structural parameter prediction with non-conventional method

DBH, Total height, crown cover and basal area was correlated and regressed with NDVI

9.4. RS & GIS Analysis:

9.4.1. Base Map preparation:

Reference topographical maps procured from SOI were mosaiced to prepare the base map for the entire Taluka. For which the map sheets were projected and tiled after digital trimming of the map boundaries. This process enabled the contiguous representation of the topographical area and the corresponding map extent.

9.4.2. Village Map Generation:

The SOI maps were also used for the generation of the village map for the study area.

9.4.3. Importing Satellite Data:

The digital data of IRS LISS III, Landsat-TM, Landsat-ETM^{+} was initially loaded into the computer hard disk in a band sequential format (BSQ), using ERDAS imagine 9.1 Image processing software. Prerequisite information such as number of pixels, rows, columns and bands was filled up while importing the data.

9.4.4. Geo-referencing: The data was geo-referenced using Geographic WGS 94 Projection

9.4.5. Sub-setting:

Using the subset utility of the ERDAS 9.1 Image software module, the exact area under the study was extracted.

9.5. Microwave data processing

Microwave data was imported in NEST 4.A environment and was subjected to other data processing techniques.

9.5.1. Need for speckle filtering

Unlike optical remote sensing images, characterized by very neat and uniform features, SAR images are affected by speckle. Speckle confers to SAR images a granular pattern with random spatial variations.

9.5.2. Filter used: Gamma filter was selected for the present study.

Gamma Map filter: This filter was first proposed by Kuan et al., 1987. The scene reflectivity was assumed to be Gaussian distributed. However, this is not quite realistic since it implicitly assumes a negative reflectivity. Lopes et al., 1990 modified the Kuan map filter by assuming a gamma distributed scene and setting up two thresholds. A prior knowledge of the probability density function of the scene is required to apply the MAP (Maximum a posteriori) approach to speckle reduction. With the assumption of a gamma distributed scene, the Gamma MAP filter is derived in the following form:

$$R = \text{Mean for } \left(SD/Mean\right) \leq \left(\sqrt{1/NLOOK}\right)$$

$$R = R_f \text{ for } \left(SD/Mean\right) < \left(\sqrt{1/NLOOK}\right) < \sqrt{\sqrt{\left(SD/Mean\right)}}$$

$$R = C_p \text{ for } \left(SD/Mean\right) \geq \sqrt{\sqrt{\left(SD/Mean\right)}}$$

where: Rf = (B*Mean + SQRT(D))/(2*A);

Mean = mean value of intensity within window;

Cp = center pixel in filter window

$$B = \left(1+\left(\sqrt{1/NLOOK}\right)^2\right) / \left(\left(SD/Mean\right)^2 - \left(\sqrt{1/NLOOK}\right)^2\right) - NLOOK-1$$

D = Mean*Mean*B*B + 4*A*NLOOK*Mean* Cp. Once the Gamma filter was generated using Erdas imagine, the backscatter values generated from filtered data were then correlated with different phenological stages and biomass levels.

9.5.3. Geo-referencing of microwave data

The ENVISAT-ASAR and Radarsat-2 data were geo-referenced with Geographic WGS-84

9.5.4. Sigma Nought (σ^o)

Backscattering coefficient is the conventional measure of the strength of radar signals reflected by a distributed scatterer, usually expressed in dB. It is a normalized dimensionless number, comparing the strength observed from the target to that expected from an area of one square meter. Sigma nought is defined with respect to the nominally horizontal plane, and in general has a significant variation with incidence angle, wavelength, and polarization, as well as with the properties of the scattering surface itself (ESA, 2005). The calibrated value can be transformed into dB units by applying 10*log10.

9.5.4.1. Retrieval of backscatter values for vegetation analysis

A 7X7 window was taken and backscatter values for different vegetation types were derived from this window.

Flow chart 2-Forest health using biochemical and biophysical parameter

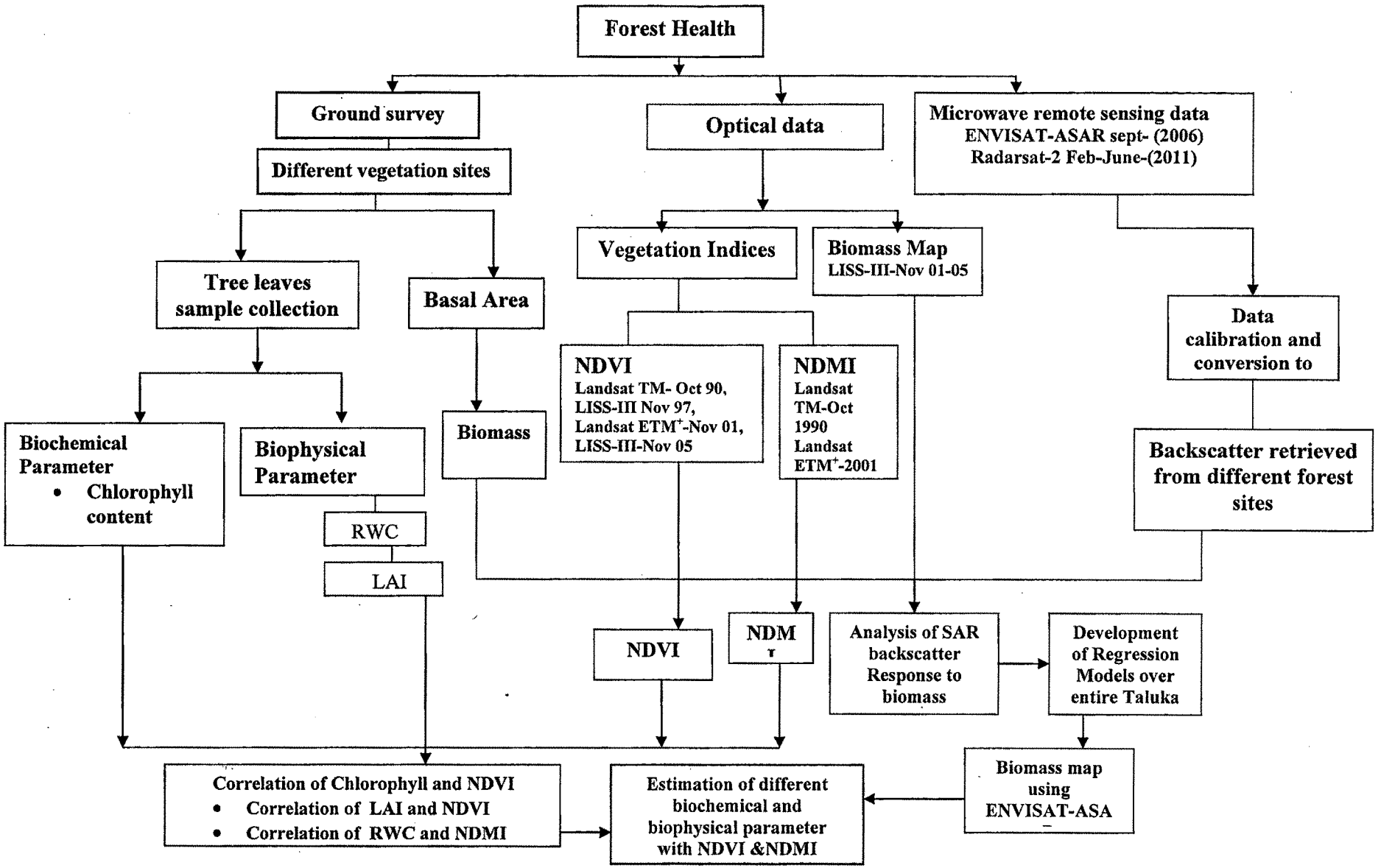

9.6. Estimation of Biochemical and Biophysical parameters

9.6.1. Conventional techniques

9.6.1.1. Estimation of chlorophyll content:

Total chlorophyll content was measured by following the method of Arnon (1949). The Arnon's equation converted absorbance measurements to mg Chl g^{-1} leaf tissue.

Chl_a (mg/g) = [(12.7 × A663) - (2.6 × A645)] × ml acetone / mg leaf tissue
Chl_b (mg/g) = [(22.9 × A645) - (4.68 × A663)] × ml acetone / mg leaf tissue
Total Chl = Chl_a + Chl_b

9.6.1.2. Estimation of Leaf area Index:

The leaf area index (LAI) is the ratio of leaf area per plant to the land area occupied by the plant and was calculated by using the formula as suggested by Sestak *et al.* (1971).

$$LAI = \frac{\text{Leaf area per plant } (m^2)}{\text{Land area occupied by a plant } (m^2)}$$

9.6.1.3. Estimation of Relative water content (RWC):

The RWC stated by Slatyer in 1967, expressed the percentage of water content in leaf tissue at a given time and specifically when the tissue are fully turgid.

$$RWC = \frac{FW - DW}{TW - DW},$$

Where, FW is the field weight, DW the oven dry weight, and TW the turgid weight.

9.6.2. Correlation of conventionally derived parameters with spatially derived indices.

9.6.2.1. Normalized difference vegetation index:

NDVI= (NIR-Red)/ (NIR+Red)

9.6.2.2. Normalized Difference Moisture Index

NDMI was derived from Landsat spectral bands 4 and 5 and was calculated using the following equation:

NDMI = *[NIR – SWIR] / [NIR+SWIR]*

9.6.2.3. Correlation of Biochemical and Biophysical parameter with Non-Conventional Data

Biochemical parameter such as chlorophyll content and Biophysical parameters such as LAI was correlated with NDVI. RWC was correlated with NDMI

9.6.3. Secondary Analysis:

Based on the forest Inventory, Biomass analysis was carried out. Basal area per hectare is an indicator of a growing stock of the forest, the approximate size of trees and standing biomass. The Biomass was calculated using the following regression equation given by Ravindranath, 1995.

Above ground Biomass (AGB)

AGB (t/ha) = -1.689 + 8.32 X BA

Where,

SE of coefficient = 1.689

$R^2 = 0.5$

BA = Basal Area in m^2/ha

9.6.4. Biomass from Optical Data

Above ground biomass through ground data was correlated to derive the regression equation. This equation was used to develop the biomass map from optical data.

9.6.5. Biomass from Microwave Data

Similarly the AGB was used to correlate the backscatter values obtained from ENVISAT ASAR was used to derive the regression equation. The ENVISAT-ASAR map was then generated using regression equation.

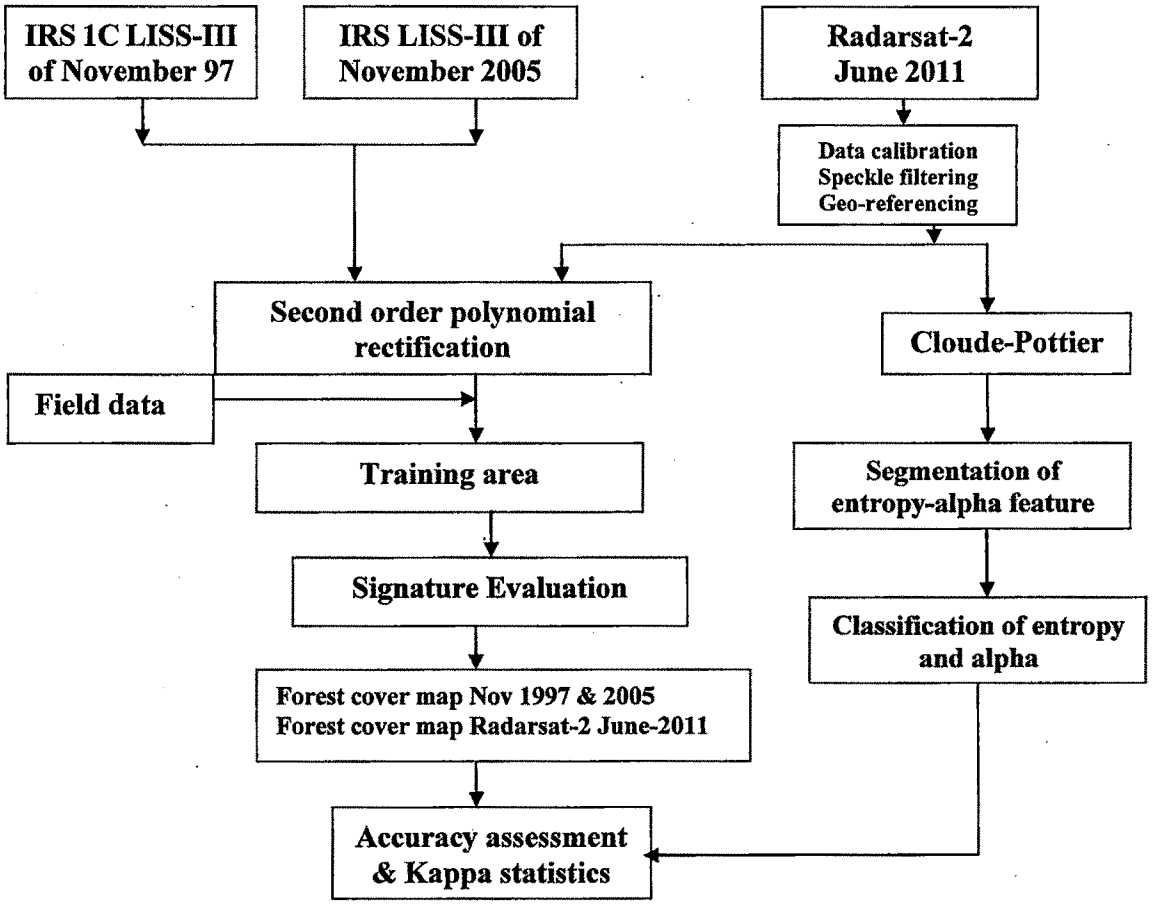

Flow chart 3Forest cover mapping using remote sensing

9.7. Techniques used for Image classification:

9.7.1. Supervised Classification for optical and microwave data

In the present study both optical and microwave data were subjected to supervised classification. This type of classification requires some knowledge about the scene, such as specific vegetative species, ground truth (field data), or data from aerial photographs or maps used to identify objects in the scene. The classification was carried using the following steps:

a) Firstly, satellite data and accompanying metadata was acquired. Information regarding platform, projection, resolution, coverage, and, importantly, meteorological logical conditions before and during data acquisition was looked for.

b) Secondly, the surface types to be mapped were chosen. Ground truth data with positional accuracy (GPS) was collected. These data were then used to develop the training classes for the discriminant analysis. Care was taken that the time of ground truth data collections to coincide with the date of data acquisition.

c) Thirdly, post-processing techniques such as corrections, image mosaics, and enhancements were performed for the image. Pixels were selected in the image that were representative (and homogenous) of the object. The Global Positioning System (GPS) data were collected, and were used for geo-referencing. The image training sites are defined by outlining the GPS polygons. The training class contained the sum of points (pixels) or polygons (clusters of pixels). The spectral histogram to inspect the homogeneity of the training classes for each spectral band was viewed. Each class was assigned a specific color. Lastly, using a discriminate analysis routine remaining pixels were extracted into the designed classes. The classified image was subjected to

accuracy assessment and was performed by using predefined ground-truth values.

9.7.2. Cloude-Pottier Decomposition

The microwave data were also classified using Cloude-Pottier decomposition. According to this theory, a target coherence matrix [T] was constructed using measurements of radar polarimetry. The coherency matrix mentioned as kp is constructed from a scattering vector in the base of Pauli that reflect geometrical properties. Usually elements of kp, are described as target vectors. It consists of horizontal or vertical components with combinations of transmitted and received SAR signals. Here, notation <...> denoted an ensemble averaging over specific neighborhood. The Cloude-Pottier theory decomposed the complex coherence matrix [T] into a set of eigenvalues (k) and eigenvectors <e>using below equation:

$$[T] = \sum_{j=1}^{3} \lambda_j \underline{e}_j \underline{e}_j^T$$

where, $\underline{e}_j = \left[\cos\alpha \quad \sin\alpha\cos\beta e^{i\delta} \quad \sin\alpha\sin\beta e^{i\gamma}\right]$

The α angle represents the types of scattering. The Beta angle (β) denotes object orientation about the line of sight. Phase difference between HH+VV and HH-VV is represented by the angle δ, while the phase difference between HH+VV and HV is represented by γ.

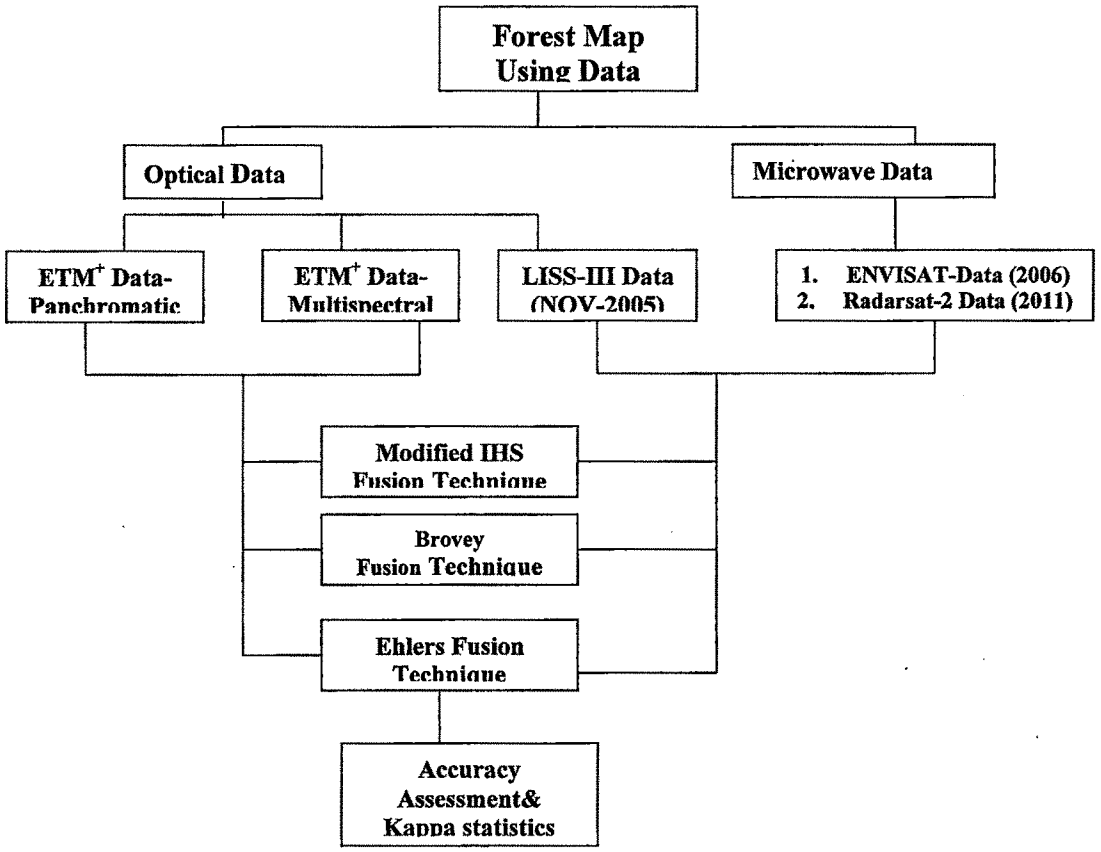

Flow chart 4 Forest Map Using Data Fusion

9.8. Data fusion Technique

In the present study optical and microwave data were fused using different data fusion techniques such as Ehlers, Modified IHS, and Brovey.

9.8.1. Ehlers Fusion Technique

In this technique the IHS transform was applied to the multispectral image.(Illustration 2) Since the IHS transform is limited to three input bands (RGB), the process is extended to include more than three bands by using multiple IHS transforms until the total number of bands is exhausted. Fourier transform is then used to enhance the spatial information. With the fast Fourier transform (FFT), the intensity channel from the IHS transform is filtered using a low pass (LP) filter and the panchromatic image (P) is filtered with an opposing high pass (HP) filter. These images are converted back into the spatial domain using an inverse fast Fourier transform (FFT^{-1}) process and added together to generate a fused intensity channel with low frequency information from the coarse spatial resolution image (via the Intensity channel) and high frequency information from the high resolution panchromatic image. An inverse IHS transformation (IHS^{-1}) is performed to produce the final fused image that contains the spatial information supplied by the panchromatic image with the spectral resolution of the multispectral image. Again, since the IHS transform is limited to using three bands, the process is extended by using multiple IHS transforms until the total number of bands are derived.

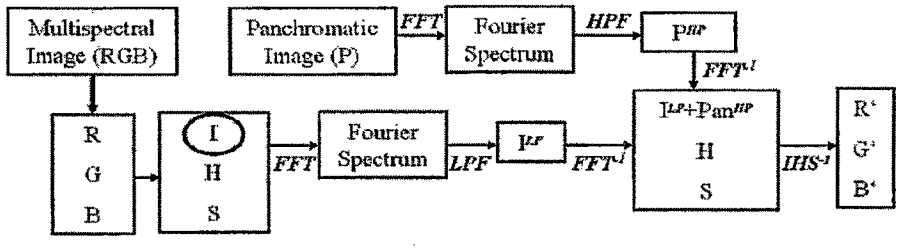

***Illustration* 2: Basic overview of the Ehlers Fusion process**

9.8.2. The Modified IHS (intensity, hue, saturation) Transformation:

This process involved the conversion of three input multispectral bands from red-green-blue (RGB) space to intensity-hue-saturation (IHS) space. The higher resolution panchromatic band was substituted for the intensity channel and the IHS transform was converted back into RGB space maintaining the panchromatic bands spatial structure.

9.8.3. Brovey Transform:

This process used a ratio algorithm to combine the multispectral and panchromatic images. The technique normalized each of the multispectral bands used and multiplied these with the higher resolution panchromatic band. When these band layers were stacked, the resultant higher resolution image was synthesized.